**This item is the archived peer-reviewed author-version of:**

Posture normalization of 3D body scans

# Posture normalization of 3D body scans

Femke Danckaers[*a], Toon Huysmans[a,b], Ann Hallemans[c,d], Guido De Bruyne[e], Steven Truijen[c,d] and Jan Sijbers[a]

[a]imec - Vision Lab, Dept. of Physics, University of Antwerp, Belgium
    Universiteitsplein 1, B-2610, Antwerp, Belgium
[b]Applied Ergonomics and Design, Faculty of Industrial Design Engineering, Delft University of Technology, The Netherlands.
    Landbergstraat 15, 2628 CE Delft, The Netherlands
[c]Multidisciplinary Motor Centre Antwerp, University Hospital Antwerp (UZA), Belgium
    Wilrijkstraat 10, B-2650 Edegem, Belgium
[d]Department of Rehabilitation Sciences and Physiotherapy, Faculty of Medicine and Health Sciences, University of Antwerp, Antwerp, Belgium
    Universiteitsplein 1, B-2610, Antwerp, Belgium
[e]Department of Product Development, Faculty of Design Sciences, University of Antwerp, Belgium
    Ambtmanstraat 1, B-2000 Antwerp, Belgium

**ABSTRACT**
For product developers that design near-body products, virtual mannequins that represent realistic body shapes, are valuable tools. With statistical shape modeling, the variability of such body shapes can be described. Shape variation captured by statistical shape models (SSMs) is often polluted by posture variations, leading to less compact models. In this paper, we propose a framework that has low computational complexity to build a posture invariant SSM, by capturing and correcting the posture of an instance. The posture-normalized SSM is shown to be substantially more compact than the non-posture-normalized SSM.

**KEYWORDS**
posture modeling; statistical shape model; 3D body scan; posture normalization

## Practitioner Summary

Statistical shape modeling is a technique to map out the variability of (body) shapes. This variability is often polluted by variations in posture. In this paper, we propose a framework to build a posture invariant statistical shape model.

## 1. Introduction

When designing wearables, realistic virtual mannequins that represent body shapes that occur in a specific target population, are valuable tools for product developers.

---

*Corresponding author: femke.danckaers@uantwerpen.be

Such tools (Digital Human Models - DHM) are already widespread, but are often an oversimplified representation of the population, based on 1D measurements, so 3D shape variation is not incorporated (Moes 2010; Blanchonette 2010; van der Meulen and Seidl 2007). That is, in DHMs, the body shape can only be modified by scaling the body parts, which is not sufficient for designing products that have to fit tightly to the body (Bragança et al. 2016).

An alternative way to capture the variability of shapes in a population is to represent these shapes by statistical shape models (SSMs) (Park and Reed 2015). Statistical shape modeling is a popular technique in 3D anthropometric analyses to map out the variability of body shapes. SSMs allow to gain a better understanding of the shape variation present in a population. By adapting the shape parameters of the model, a new, realistic shape can be formed. The user may exploit SSMs by using them as virtual design mannequins and analyze the body shapes that belong to (a percentile of) a target group. This is highly valuable for designers who want to create near-body products for a specific target population. In that way, it is possible to visualize extreme body shapes. Moreover, an SSM allows to simulate a specific 3D body shape (Park et al. 2015), which is useful for customization in a (possibly automated) workflow.

When scanning people in standing pose, posture differences may occur over the population. If SSMs are built from these scans, body posture will have a significant and often undesired influence on the shape modes. Even when the individuals are instructed to stand still in a specific pose, slight posture changes are unavoidable, especially in the region of the arms. As a result, some shape variances are unintentionally correlated with posture. Posture variety is, for example, also present in the Civilian American and European Surface Anthropometry Resource (CAESAR) database (Robinette, Daanen, and Paquet 1999). In addition, this results in a non-compact model, as posture variances can be regarded as extra degrees of freedom that are not interesting when analyzing shape variances. Therefore, it is less suitable for e.g. classification applications for creating a sizing system, where a new subject is assigned to a specific body shape group. Furthermore, the computational cost when using a compact SSM will be significantly lower compared to that of a non-compact model as more modes are necessary to describe the population variation. A less compact SSM needs more parameters to describe a certain percentage of variation in the population, so this model will be more complex for e.g. classification applications.

The main goal of this paper is to construct posture invariant SSMs from a set of 3D body scans. Most posture normalization techniques are based on rotation and translation of the separate body parts, such as arms and legs. In particular, linear blend skinning (LBS) is a popular technique (Baran and Popović 2007). In LBS, the surface mesh is linked to a simplified skeleton consisting of joints and bones. Thereby, posture is commonly normalized by transforming each bone separately. For every bone of the skeleton, a smooth weight map is assigned to the vertices of the 3D body shape. The vertices are subsequently transformed along with the bone and relative to the assigned weights. To normalize a shape, the skeleton has to be transformed to the optimal bone angles. The disadvantage of LBS is that it may result in an unnatural body shape, because LBS cannot compensate for muscle bulging (except when introducing helper bones, which is cumbersome) and joint rotations may produce a collapsing effect where the skin collapses to a single point, also known as the candy-wrapper artifact (Mohr and Gleicher 2003).

Wuhrer, Shu, and Xi (2012) and Pishchulin et al. (2017) applied a posture-invariant shape analysis of body shapes using the Laplace operator, separating the shape space from the posture space. They optimized the Laplacian coordinates of the average shape

2

of the model to minimize the distance to every corresponded input shape. This leads to meshes that have the body shape of the input shape and the posture of average shape. This technique is computationally expensive for surface meshes with many vertices, because for every vertex an optimization problem needs to be solved.

The SCAPE method (Anguelov et al. 2005) is a data-driven method that assumes the body shape and posture to be uncorrelated. This technique generates more realistic body shapes, as even muscle bulging is simulated. However, by considering shape and pose deformations separately, it is not accurate since pose deformation is person-dependent. Another drawback of SCAPE is that it is time-consuming (compared to e.g. LBS) as a least-squares system needs to be solved in order to reconstruct a surface from pose and shape parameters. On the other hand, Chen, Liu, and Zhang (2013) generated a tensor-based model, which jointly models shape and pose deformations. The resulting surfaces look more realistic after pose deformation compared to using the SCAPE method. Reed, Park, and Corner (2016) developed a pose modification technique by calculating a mapping matrix between two SSMs of the same population in a different pose. However, the posture of the input shapes has a high influence on their results. By first applying posture normalization, more accurate results are obtained by pose modification.

We propose a fast, skeleton-less, data-driven method to perform statistical shape modeling in a posture invariant way by minimizing the influence of posture. This work is an extension of previous, preliminary research of the authors (Danckaers et al. 2018). An extreme posture normalization experiment is added. Furthermore, a feature analysis to determine the optimal features to predict a body shape from features is conducted. Therefore, a shape prediction test was applied to 20 subjects, with every possible combination of 14 easy to obtain features. We also created a color map that shows the distribution of prediction errors on the whole body shape. From these experiments, the optimal features for posture normalization were deduced. Lastly, an extensive discussion about the results was added.

## 2.    Methods

In this section, the proposed framework to obtain posture invariant SSMs is described. The flow-chart of this framework is illustrated in Figure 1. First, from a population of 3D human body shapes, an SSM is built (Danckaers et al. 2014). Next, the appearance of every shape is modified so that its new features are equal to those of the average shape. This process is called identity removal. Then, the feature normalization technique is described. From the resulting identity low shapes, a posture model is built, which captures the variation of postures throughout the input population. If such a model is registered to a new input shape, then only posture is retained. Next, the deformation from the captured posture to the average posture, defined as the posture of the average shape, is computed and subtracted from the input shape, which results in a posture-normalized shape (Danckaers et al. 2018).

### 2.1.    *Statistical Shape Model*

Every shape in the population is represented by a mesh consisting of $n$ vertices. If a population consists of $N$ shapes in the population, it can be represented by a $3n$-dimensional point cloud, consisting of $N$ points, where every point represents a shape. By applying principal component analysis (PCA) on the point cloud, the population
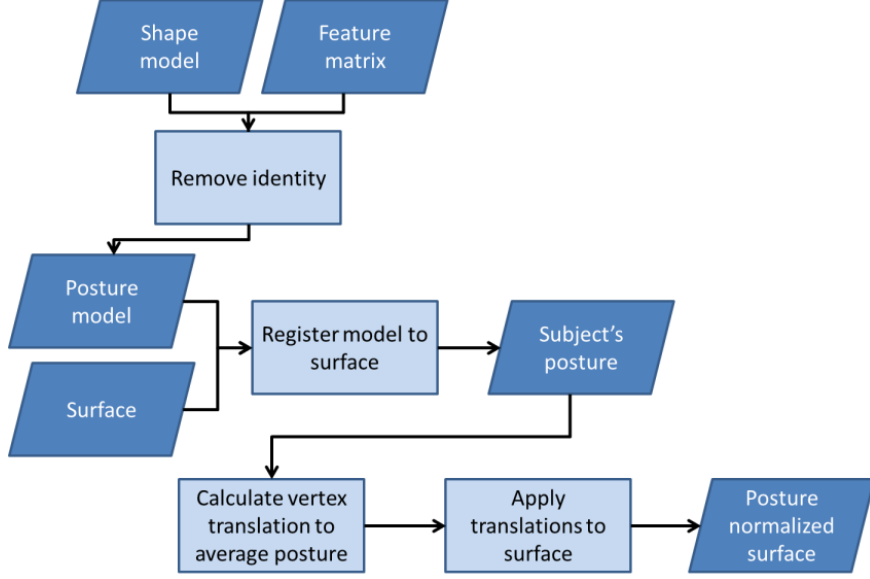
**Figure 1.** The proposed framework for building posture invariant SSMs.

is represented by a mean point (which represents the mean shape) and $N - 1$ eigenmode vectors. The largest shape variance in the population is represented by the first eigenmode vector. Perpendicular to that vector is the vector that describes the second largest shape variance, etc. The mean shape $\bar{\mathbf{x}} \in \mathbb{R}^{3n}$ and the main principal component (PC) modes $\mathbf{P}_s \in \mathbb{R}^{3n \times (N-1)}$ are incorporated in the SSM. By adding a linear combination of the PCs to the mean shape, a new shape $\mathbf{y} \in \mathbb{R}^{3n}$ can be generated. Note that this shape will always lie within the shape space of the SSM.

$$\mathbf{y} = \bar{\mathbf{x}} + \mathbf{P}_s \mathbf{b}, \tag{1}$$

with $\mathbf{b} \in \mathbb{R}^{N-1}$ the vector containing the SSM parameters.

### 2.2. *Feature Modification*

An SSM is a mathematical model that can be controlled by parameters. A specific body shape can be adapted by adding a linear combination of parameters to that individual's shape vector. These parameters do not necessarily have a physical meaning. A more intuitive way of adjusting a body shape, is linking those parameters to physical features, such as height, weight, gender,... so the body shape is adaptable by changing the feature values.

Feature modification is done by applying multiple linear regression on the PC weights and the shape specific features of every body shape in the population (Danckaers et al. 2015). It is important to know which features influence body shape to generate an accurate posture model.

Let $\mathbf{f}_i = [f_1 f_2 \cdots f_F 1]^T \in \mathbb{R}^{F+1}$ be the feature vector that contains the $F$ known features of a specific body shape and $\mathbf{b}_i \in \mathbb{R}^{N-1}$ the shape specific PC weights. Suppose that these features of every shape $i$ from the dataset are known, so $\mathbf{B} = [\mathbf{b}_1 \mathbf{b}_2 \cdots \mathbf{b}_N] \in \mathbb{R}^{(N-1) \times N}$ is the matrix containing the PC weights of each surface, while $\mathbf{F} = [\mathbf{f}_1 \mathbf{f}_2 \cdots \mathbf{f}_N] \in \mathbb{R}^{(F+1) \times N}$ is the matrix containing the features

of each surface. That means that a mapping matrix $\mathbf{M} \in \mathbb{R}^{(N-1) \times (F+1)}$, describing the relationship between the PC weights matrix $\mathbf{B}$ and the feature matrix $\mathbf{F}$ can be calculated by

$$\mathbf{M} = \mathbf{B} \mathbf{F}^{+}, \tag{2}$$

with $\mathbf{F}^{+}$ being the pseudoinverse of $\mathbf{F}$. Using this mapping matrix, the PC weights $\mathbf{b}$ of a body shape with features $\mathbf{f}$ can be generated by

$$\mathbf{b} = \mathbf{M} \mathbf{f}. \tag{3}$$

### 2.3. *Identity Removal*

The identity of a surface is the shape characteristics that represent a specific person and can be quantified by the feature values. By removing the identity of each body scan, shape specific deformations are filtered out and only posture related deformations remain. To do so, the features of each shape are modified in a way that they are equal to the features of the average shape of the dataset, resulting in similarly looking shapes. In what follows, we will refer to these shapes as identity-free shapes.

First, the specific PC weight vector $\mathbf{b}_i$ of instance $i$ is extracted from the PC matrix $\mathbf{B}$. Then, the features that should be added to the current features of instance $i$ to obtain equal values as the average features are calculated and stored in the delta feature vector $\Delta \mathbf{f}$ by extracting the specific features $\mathbf{f}_i$ (defined as the $i$th column of $\mathbf{F}$) of instance $i$ from the average features $\bar{\mathbf{f}}$ of the population:

$$\Delta \mathbf{f} = \bar{\mathbf{f}} - \mathbf{f}_i. \tag{4}$$

Next, the delta PC weights vector $\Delta \mathbf{b}$ that represent the displacement of every vertex from the original body shape to the identity-free body shape, is calculated by multiplying the mapping matrix $\mathbf{M}$ with the previously calculated delta features $\Delta \mathbf{f}$:

$$\Delta \mathbf{b} = \mathbf{M} \cdot \Delta \mathbf{f}. \tag{5}$$

These delta PC weights $\Delta \mathbf{b}$ are subsequently added to the original PC weights $\mathbf{b}_i$ to obtain the PC weights $\mathbf{b}_i'$ of the identity-free body shape:

$$\mathbf{b}_i' = \mathbf{b}_i + \Delta \mathbf{b}. \tag{6}$$

Finally, the identity-free body shapes, $\mathbf{x}_i'$, are calculated by multiplying the identity-free PC weights $\mathbf{b}_i'$ with the PC vectors $\mathbf{P}_s$ of the SSM and adding the result to the mean shape $\bar{\mathbf{x}}$:

$$\mathbf{x}_i' = \bar{\mathbf{x}} + \mathbf{P}_s \mathbf{b}_i'. \tag{7}$$

From the set of shapes without identity, a new SSM is built (Danckaers et al. 2014) that represents a posture model. The result is a posture model, whose variances are mainly the posture variances that are present inside the population.

### 2.4. *Posture Normalization*

The posture of a body shape is normalized by corresponding that shape with the statistical posture model, as described in Danckaers et al. (2014). Note that the posture model and the new shape do not have to stem from the same dataset. It is sufficient that they have roughly the same pose. From the corresponded posture model, the PC weights of that body shape are calculated. In the posture model mainly posture variations are captured.

Before normalizing the shape $\mathbf{x}_i$, it is scaled to match the height of the posture model. Next, the inverse PC matrix $\mathbf{P}_p$ of the posture model is multiplied by the vector that holds the distance between every vertex of the input surface and the mean surface mesh $\bar{\mathbf{x}}$ to obtain the posture PC weights $\mathbf{b}_i$ $\bar{\mathbf{x}}$. Note that these posture PC weights describe only the differences in posture compared to the mean posture.

$$\mathbf{b}_i = \mathbf{P}_p^T(\mathbf{x}_i - \bar{\mathbf{x}}). \tag{8}$$

Next, the posture $\mathbf{x}_i'$ of the input shape is reconstructed from the calculated posture PC weights $\mathbf{b}_i$:

$$\mathbf{x}_i' = \bar{\mathbf{x}} + \mathbf{P}_p \mathbf{b}_i \tag{9}$$

Finally, the normalized shape $\hat{\mathbf{x}}_i$ is calculated by subtracting the posture influence $\mathbf{P}_p \mathbf{b}_i$ on the shape from the original shape $\mathbf{x}_i$:

$$\hat{\mathbf{x}}_i = \mathbf{x}_i - \mathbf{P}_p \mathbf{b}_i. \tag{10}$$

In case the user wants to correct a shape to a posture that differs from the average posture, it suffices to calculate the PC weights $\mathbf{b}^*$ of that specific posture and subsequently calculate the posture corrected shape $\check{\mathbf{x}}$ as follows:

$$\check{\mathbf{x}} = \mathbf{x}_i - \mathbf{P}_p(\mathbf{b}_i - \mathbf{b}^*). \tag{11}$$

## 3. Results

Our proposed posture normalization algorithm was applied to shapes from the Dutch CAESAR database (Robinette, Daanen, and Paquet 1999). This is an extensive database that contains 3D scans, measurements and other meta-data of over 1000 people in standing pose. All subjects were scanned using the Vitronic Vitus Pro laser scanner (Vitronic 1994) with a resolution of $2mm \times 2mm \times 2mm$ and a point density of 300 points/$cm^3$. Although the scanned persons were instructed to take a specific pose, posture variations are present in the CAESAR database.

In the following subsections, an SSM in standing pose is built and the different steps to build a posture-normalized SSM are illustrated. The compactness of the non-normalized model is compared to the compactness of the normalized model and an optimal set of features for posture normalization was calculated.

6

### 3.1. *Statistical Shape Model*

To validate the algorithm, an SSM of a population of 700 body shapes (350 men, 350 women) in standing pose was built. Every 3D scan was registered by the same 3D body shape, which was digitally modeled and consists of 100k uniformly distributed vertices (Valette, Chassery, and Prost 2008).

The first three PC modes of the unmodified SSM are shown in Figure 2. In the third mode, influence of posture is clearly noticeable.

### 3.2. *Posture-normalized Shape Model*

In Figure 3, two examples of identity removal are shown. The resulting shapes look more similar than the original shapes. The features that were used for identity removal are: gender, acromial height sitting, ankle circumference, spine-to-shoulder, spine-to-elbow, arm length (spine to wrist), arm length (shoulder to wrist), arm length (shoulder to elbow), armscye circumference (scye circumference over acromion), bizygomatic breadth, chest circumference, bust/chest circumference under bust, buttock-knee length, chest girth (chest circumference at scye), crotch height, elbow height sitting, eye height sitting, face length, foot length, hand circumference, hand length, head breadth, head circumference, head length, hip breadth sitting, hip circumference maximum, hip circumference max height, knee height, neck base circumference, shoulder breadth, sitting height, stature, subscapular skinfold, thigh circumference, thigh circumference max sitting, thumb tip reach, TTR 1, TTR 2, TTR 3, triceps skinfold, crotch length, vertical trunk circumference, waist circumference preferred, waist front length, waist height preferred, weight.

In Figure 4, the posture model is shown. The number of shape modes was restricted to the first 12 to reduce noise, such as variations that were more due to variations in body shape than variations in posture. This number was determined by manually inspecting the shape modes. Then, the posture of every input shape of the non-normalized SSM was corrected. From the normalized shapes a new, posture normalized SSM was built. In Figure 5, the first three shape modes of this posture normalized SSM are shown.

### 3.3. *Posture Normalization Case*

Six instances of the same shape with slightly different postures were artificially generated by rotating skeleton parts and applying linear blend skinning (Baran and Popović 2007) on the shape. Then, for every modified shape, the posture was normalized. The resulting deformed and normalized instances are shown in Figure 6. The average distance between the posture normalized shapes was $(2.91 \pm 0.99)mm$. Normalizing the posture of a shape took around $10s$ on a computer with an Intel Core i7-5960X CP @ 3.00GHz processor and 32 GB memory.

### 3.4. *Model Performance - Compactness*

Compactness is a widely used measure for quantifying the correspondence quality of an SSM (Davies et al. 2002; Su 2011). A compact SSM is a model that has as little variance as possible and requires as few parameters as possible to define an instance. This suggests that the shape variance is captured in a plot of cumulative variance. Therefore
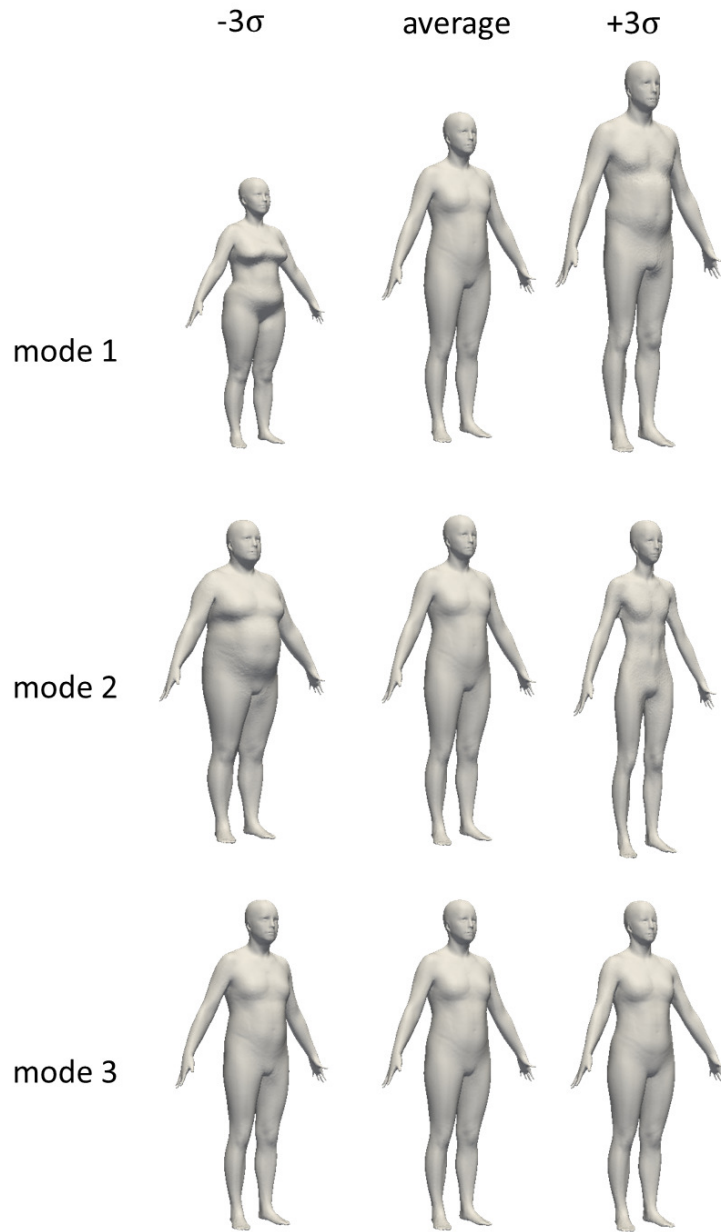
**Figure 2.** The first three eigenmodes of the non-normalized SSM, built from the non-normalized shapes. In the third mode posture variation is clearly noticeable, as the main shape variation is the position of the arms and shoulders.
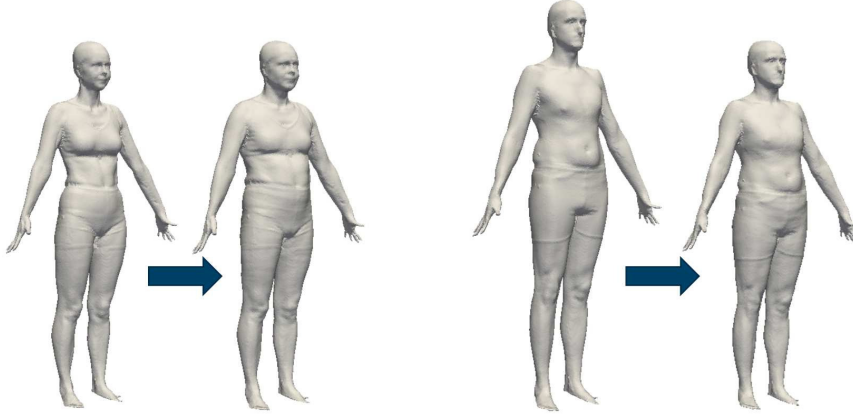
**Figure 3.** Two examples of identity removal. Mainly posture differences remain, as the body features are averaged out.

calculation time decreases significantly when using the SSM for shape prediction from parameters, for example (Danckaers et al. 2015). The compactness $C(m)$ is expressed as the sum of variances of the SSM using $m$ shape modes,

$$C(m) = \sum_{i=1}^{m} \lambda_i, \tag{12}$$

where $\lambda_i$ is the variance in mode $i$.

Figure 7 shows the compactness as a function of the number of shape modes. The graphs show that the normalized SSM is a more compact representation of the population compared to the non-normalized SSM. The non-normalized SSM can describe over 90% of the shape variation present in the population using seven shape modes. However, for the non-normalized SSM two shape modes are already sufficient to describe the same amount of shape variation. The normalized SSM is 16% more compact compared to the non-normalized SSM, when using only one shape mode. Using five shape modes, the normalized SSM was 23% more compact. When using ten shape modes, an improvement of 25% was obtained. In general, the normalized SSM performs better in terms of compactness and a greater proportion of shape variance is captured in the first modes of the normalized SSM.

### 3.5. *Feature Selection*

An optimal set of features to predict a body shape was selected by cross-validation. The importance of each feature for predicting a body shape was determined by simulating a body shape based on features and comparing this shape with the real shape. The CAESAR database contains a lot of meta-data that do not necessarily influence the body shape. In this paper, for posture normalization, we used all available data. Missing meta-data in the CAESAR database were estimated through imputation on the whole dataset (Wold 1973).

The test was applied to 20 non-normalized shapes (10 men and 10 women) for the 14 easiest to measure features, using only a balance and a tape measure: gender (G), age (A), arm length (AL), breast circumference (BC), chest circumference (CC), crotch
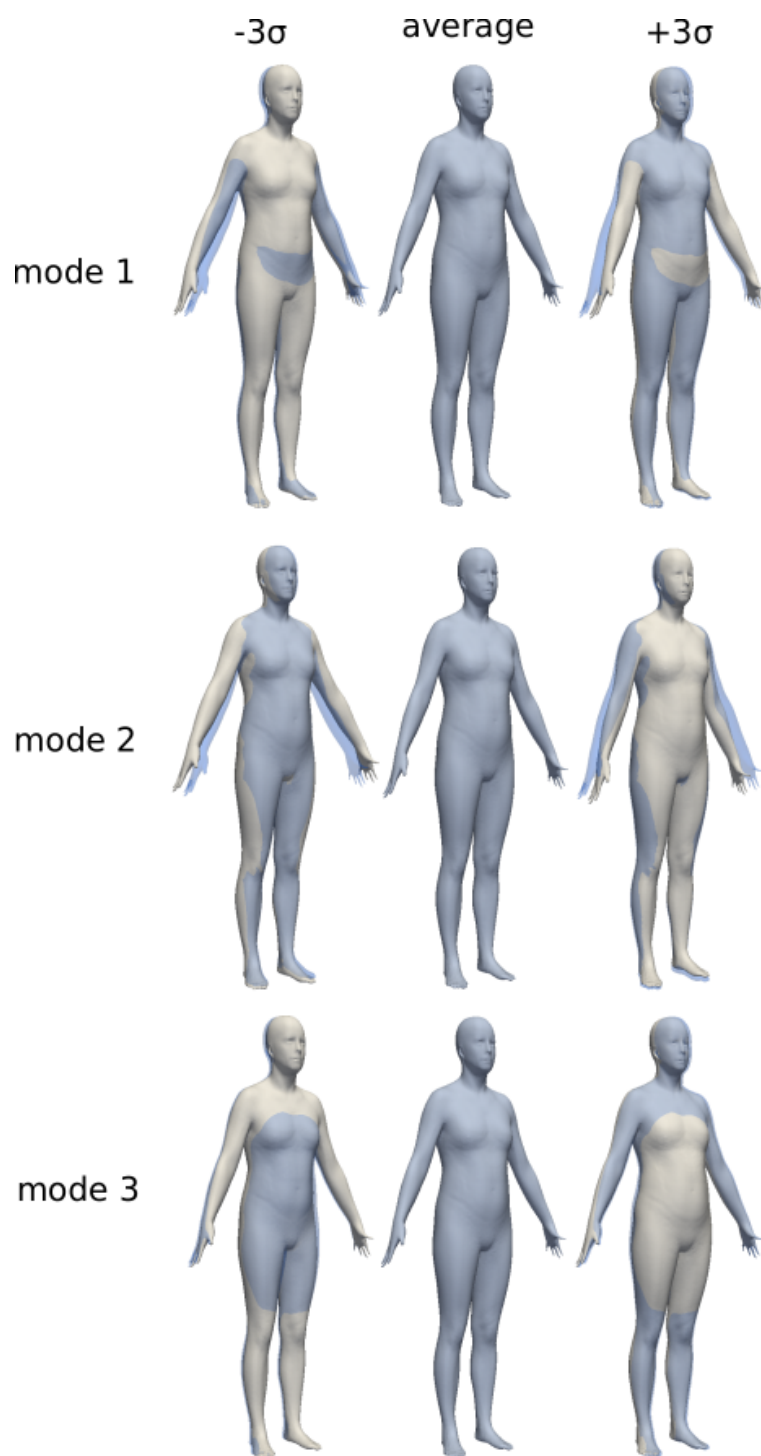
**Figure 4.** The first three eigenmodes of the posture model. In the regions of the arms and the torso, posture variation is noticeable. To better visualize the posture variations, the shapes are overlaid with the average shape in blue.
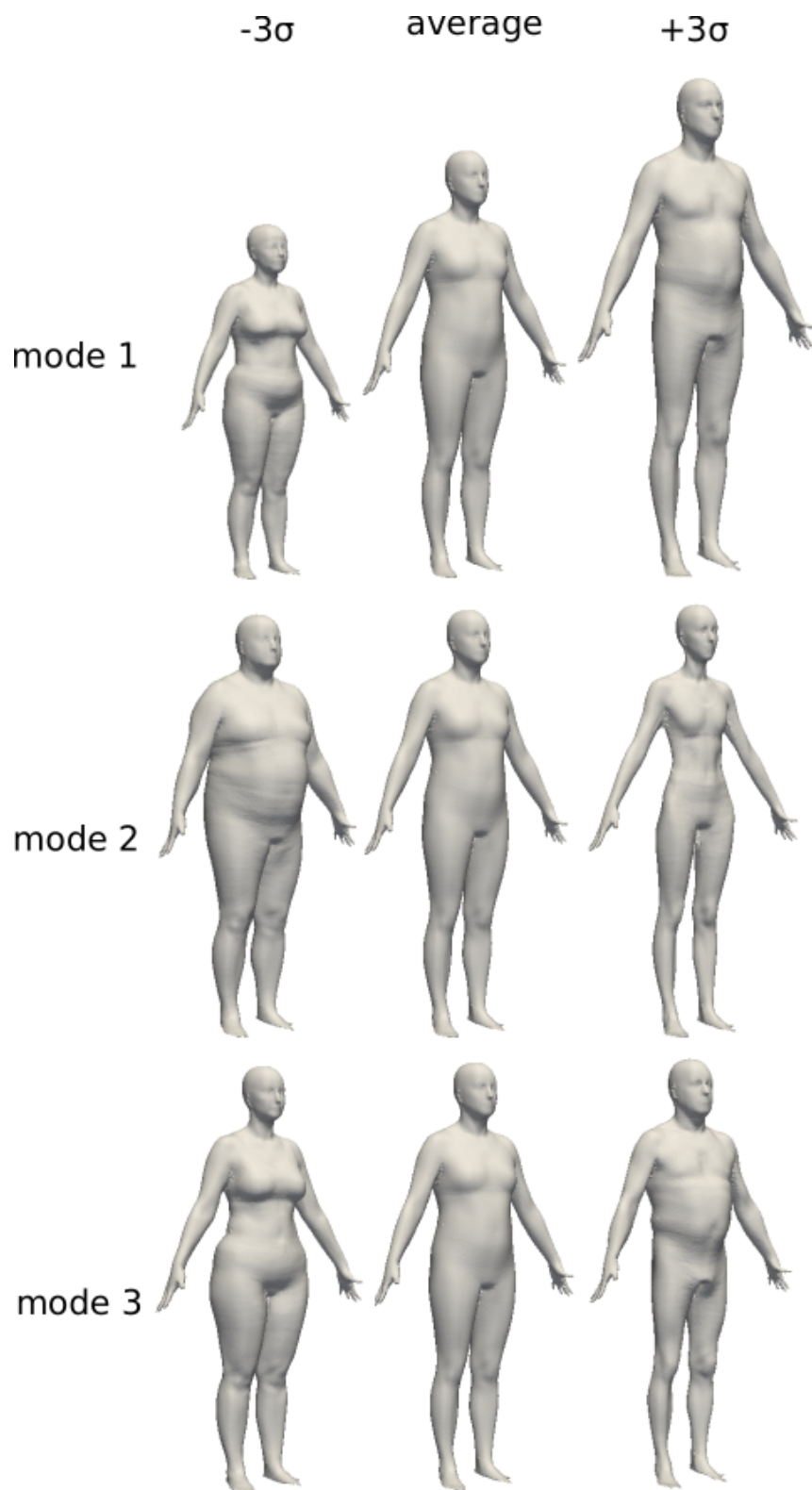
10

**Figure 5.** The first three eigenmodes captured by the posture normalized SSM. In this SSM, the shape variances of the body are better captured compared to the shape modes that came out of the non-normalized SSM (see Figure 2. In this normalized SSM, the third eigenmode mainly describes gender. In comparison, the third eigenmode of the non-normalized SSM mainly describes the position of the arms.
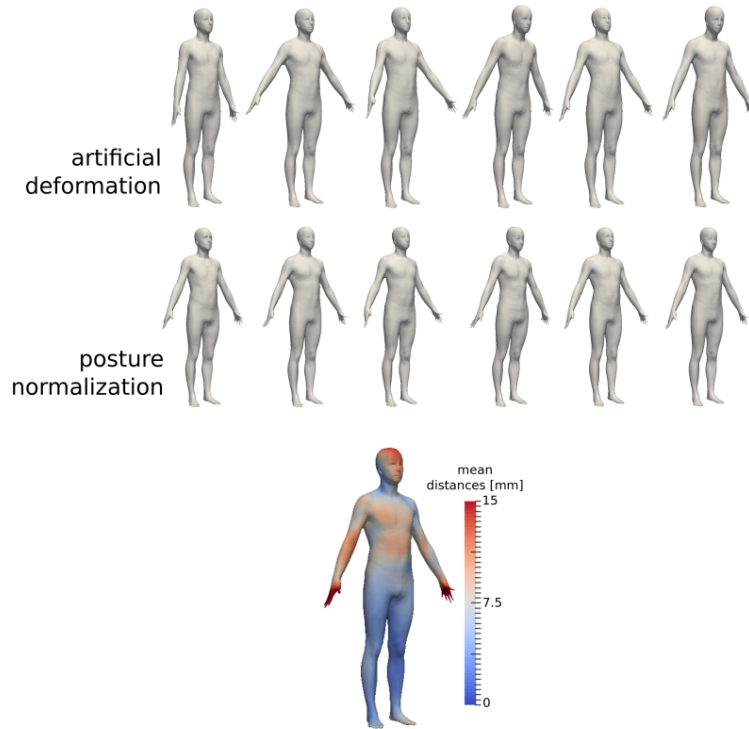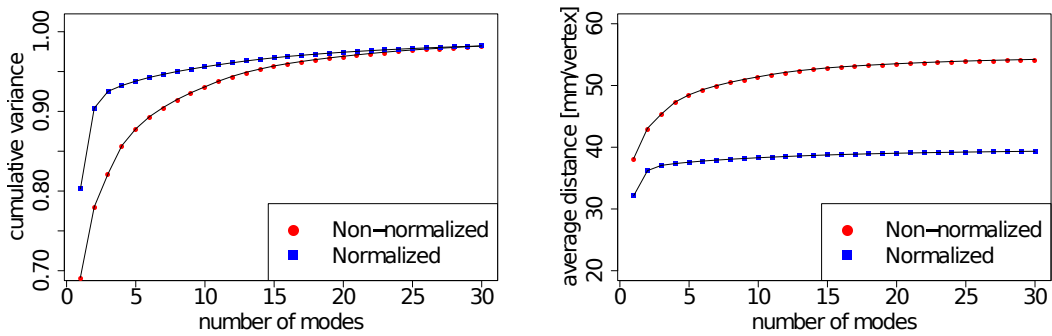
**Figure 6.** Posture normalization case. Top row: The same input shape was artificially deformed by rotating skeleton parts and applying LBS. Bottom row: the result of the posture normalization algorithm. The average distance between the posture normalized shapes and the original (non-modified) shape is shown below in $mm$/vertex, mapped on the ground truth.



(a) The average deviation from the mean shape of a shape described by a specific number of shape modes is shown.

(b) The average deviation from the mean shape of a shape described by a specific number of shape modes is shown in mm/vertex.

**Figure 7.** Compactness graphs: the cumulative variance (a) and average distance (b) as a function of the number of shape modes.

(a) Regular non-normalized SSM, in mm/vertex. The largest errors appear in the regions of the arms and the head, due to posture differences.

(b) Posture normalized SSM, in mm/vertex. The largest errors appear in the stomach region. The previously noticeable errors in the regions of the arms and the heads are strongly reduced.
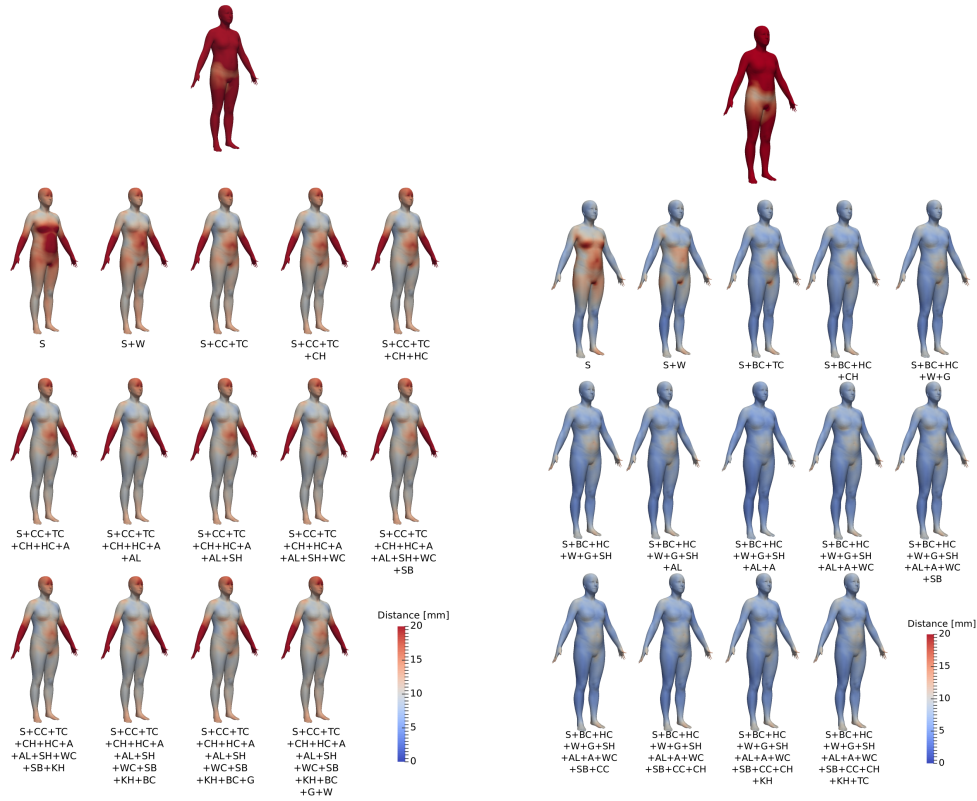
**Figure 8.** Color map that denotes the average distance between the shape predicted from a set of features and true shape.

height (CH), hip circumference (HC), knee height (KH), shoulder breadth (SB), sitting height (SH), stature (S), thigh circumference (TC), waist circumference (WC), and weight (W). For every test subject, the body shape was predicted from every possible combination of its features. The average distance per vertex from the predicted body shape to the true body shape is calculated. The results are shown in Table 1. From a set of five features on, there is little improvement noticeable.

The average distance is visualized for every set of features on the average body shape and visualized in Figure 8. These results show that the largest errors occur in the region of the arms and the head. This is due to posture related differences in the dataset. This test was repeated with the posture normalized SSM. The results are shown in Table 2 and Figure 8.

### 3.5.1. Posture Normalization with a Small Set of Features

From the complete set of features included in the CAESAR database a posture model was built. To validate the influence of the used number of features on posture normalization, the experiment was repeated for the best feature set using 5 features and the best feature set using 11 features, selected from the 14 easiest to measure features. The posture models are shown in Figure 9.

**Table 1.** Average distance from the predicted body shape to the true shape using the non-normalized SSM, in mm/vertex. Only the two best results per number of features is shown. The test was applied for the 14 most relevant features: gender (G), age (A), arm length (AL), breast circumference (BC), chest circumference (CC), crotch height (CH), hip circumference (HC), knee height (KH), shoulder breadth (SB), sitting height (SH), stature (S), thigh circumference (TC), waist circumference (WC), and weight (W). The best set of features is marked in bold. Note that the last feature of the second best combination using $n$ features is the last feature of the best combination using $n+1$ features.

| | Features | Average distance [mm] |
|---|---|---|
| 0 | | 31.17 ± 18.01 |
| 1 | S | 15.44 ± 3.27 |
| | SH | 18.22 ± 3.78 |
| 2 | S + W | 13.99 ± 2.92 |
| | S + CC | 14.04 ± 3.00 |
| 3 | S + BC + TC | 13.14 ± 2.80 |
| | S + BC + HC | 13.22 ± 2.73 |
| 4 | S + BC + TC + CH | 13.01 ± 2.81 |
| | S + BC + TC + HC | 13.01 ± 2.70 |
| 5 | S + BC + TC + CH + HC | 12.86 ± 2.69 |
| | S + BC + TC + CH + A | 12.90 ± 2.73 |
| 6 | S + BC + TC + CH + HC + A | 12.75 ± 2.58 |
| | S + BC + TC + CH + HC + AL | 12.78 ± 2.57 |
| 7 | S + BC + TC + CH + HC + A + AL | 12.68 ± 2.46 |
| | S + BC + TC + CH + HC + A + SB | 12.69 ± 2.52 |
| 8 | S + BC + TC + CH + HC + A + AL + SH | 12.65 ± 2.45 |
| | S + BC + TC + CH + HC + A + AL + WC | 12.65 ± 2.47 |
| 9 | S + BC + TC + CH + HC + A + AL + SH + WC | 12.62 ± 2.44 |
| | S + BC + TC + CH + HC + A + AL + SH + SB | 12.63 ± 2.42 |
| 10 | S + BC + TC + CH + HC + A + AL + SH + WC + SB | 12.60 ± 2.41 |
| | S + BC + TC + CH + HC + A + AL + SH + WC + KH | 12.61 ± 2.56 |
| 11 | **S + BC + TC + CH + HC + A + AL + SH + WC + SB + KH** | **12.59 ± 2.53** |
| | S + BC + TC + CH + HC + A + AL + SH + WC + SB + CC | 12.62 ± 2.46 |
| 12 | S + BC + TC + CH + HC + A + AL + SH + WC + SB + KH + CC | 12.62 ± 2.55 |
| | S + BC + TC + CH + HC + A + AL + SH + WC + KH + CC + G | 12.65 ± 2.54 |
| 13 | S + BC + TC + CH + HC + A + AL + SH + WC + SB + KH + CC + G | 12.66 ± 2.54 |
| | S + BC + TC + CH + HC + A + AL + SH + WC + SB + KH + CC + W | 12.79 ± 2.55 |
| 14 | S + BC + TC + CH + HC + A + AL + SH + WC + SB + KH + CC + G + W | 12.83 ± 2.55 |

**Table 2.** Average distance from the predicted body shape to the true shape using the posture-normalized SSM, in mm/vertex. Only the best result per number of features are shown. The most important features to predict a person's body shape. The test was applied for the 14 most relevant features: gender (G), age (A), arm length (AL), breast circumference (BC), chest circumference (CC), crotch height (CH), hip circumference (HC), knee height (KH), shoulder breadth (SB), sitting height (SH), stature (S), thigh circumference (TC), waist circumference (WC), and weight (W). The best set of features is marked in bold.

| | Features | Average distance [mm] |
|---|---|---|
| 0 | S | $26.67 \pm 20.04$ |
| 1 | S | $10.09 \pm 2.84$ |
| | KH | $14.07 \pm 5.81$ |
| 2 | S + W | $8.08 \pm 1.54$ |
| | S + BC | $8.16 \pm 1.62$ |
| 3 | S + BC + HC | $7.11 \pm 1.20$ |
| | S + W + HC | $7.14 \pm 1.42$ |
| 4 | S + BC + HC + CH | $6.94 \pm 1.14$ |
| | S + BC + HC + G | $6.94 \pm 1.30$ |
| 5 | S + BC + HC + W + G | $6.84 \pm 1.30$ |
| | S + BC + HC + SH + G | $6.85 \pm 1.35$ |
| 6 | S + BC + HC + W + CC + SH | $6.75 \pm 1.32$ |
| | S + BC + HC + W + G + SH | $6.75 \pm 1.35$ |
| 7 | S + BC + HC + W + CC + SH + AL | $6.67 \pm 1.31$ |
| | S + BC + HC + W + G + SH + AL | $6.67 \pm 1.35$ |
| 8 | S + BC + HC + W + G + SH + AL + A | $6.63 \pm 1.30$ |
| | S + BC + HC + W + CC + SH + AL + A | $6.63 \pm 1.34$ |
| 9 | S + CC + HC + W + G + SH + AL + A + WC | $6.61 \pm 1.30$ |
| | S + BC + HC + W + G + SH + AL + A + WC | $6.61 \pm 1.35$ |
| 10 | S + BC + HC + W + G + SH + AL + A + WC + SB | $6.60 \pm 1.27$ |
| | S + BC + HC + W + G + SH + AL + A + WC + CC | $6.60 \pm 1.31$ |
| 11 | S + BC + HC + W + G + SH + AL + A + WC + SB + CC | $6.59 \pm 1.28$ |
| | S + BC + HC + W + G + SH + AL + A + WC + SB + CH | $6.60 \pm 1.23$ |
| 12 | **S + BC + HC + W + G + SH + AL + A + WC + SB + CC + CH** | **$6.59 \pm 1.24$** |
| | S + BC + HC + W + G + SH + AL + A + WC + SB + CC + TC | $6.62 \pm 1.29$ |
| 13 | S + BC + HC + W + G + SH + AL + A + WC + SB + CC + CH + TC | $6.63 \pm 1.26$ |
| | S + BC + HC + W + G + SH + AL + A + WC + SB + CC + CH + KH | $6.65 \pm 1.26$ |
| 14 | S + BC + HC + W + G + SH + AL + A + WC + SB + CC + CH + KH + TC | $6.69 \pm 1.28$ |

15

The first three modes are similar for every set of features. However, in the seventh shape mode, a difference in shape is noticeable. This has influence on posture normalization, as those shape differences will be filtered out.

## 4. Discussion

The main innovation presented in this paper is a thorough evaluation of a new methodology to generate posture invariant statistical shape models. Consequently, shape variation of a human 3D body scan population can be analyzed in a more precise way. The shapes were described in a detailed, realistic way and focus mainly on shape variation, compared to the current SSMs where posture variation is incorrectly regarded as shape variation. The algorithm is applicable to any body shape of any dataset, standing in A-pose. No prior knowledge of shape dimensions is required when a posture model is already available. With a posture model available, it took $10s$ to normalize a body shape.

An important advantage of a posture normalized model is that the posture remains consistent for all generated body instances using the SSM. For product designers that use the model to generate design mannequins, it is preferred to keep a constant posture for different body shapes. Shape and posture are treated as two different things when designing, so it is a benefit to be able to regard them as two separate things when creating a virtual mannequin as well. By separating posture from body shape, a designer can start from the same preconditions for designing for different sizes. Hence, a designer can link a virtual design to the SSM so the design changes along with the body shape. Furthermore, the shape modes are easier to interpret and can be linked to specific features, which in turn may simplify shape prediction. Additionally, with a posture normalized SSM, clustering will not be polluted by posture, as the 3D coordinates of corresponding points are closer to each other, so it is less likely that shapes with similar posture will unintended be regarded as similar shapes.

The posture model itself, on the other hand, can be a valuable tool to validate a design. The posture variation captured by the posture model can be used to vary the posture of a generated mannequin. In that way, the designer has full control over the posture and shape of the design manikins and can use this control to systematically validate his designs with respect to natural posture and shape variations.

The normalized SSM is a more compact representation of the population compared to the non-normalized SSM. For example, to describe over 90% of the shape variation present in the population, the non-normalized SSM requires seven shape modes, while only two shape modes are sufficient to describe the same amount of variation for the normalized SSM. The normalized SSM is 16% more compact using one shape mode, compared to the non-normalized SSM. For five shape modes, an improvement of 23% was seen. Using ten shape modes, an improvement of 25% was observed. A compact model has many advantages. It will decrease the need for storage space. Indeed, if almost all of the variance is captured by $K$ modes with $K << N$, only $K$ rows of matrix $B \in \mathbb{R}^{(N-1) \times N}$ need to be stored. Another advantage of a compact model, is that less computation time is consumed when using the model for applications such as shape prediction. The complexity of calculating mapping matrix $\mathbf{M} = \mathbf{B}\mathbf{F}^+$, with principal component (PC) weights matrix $\mathbf{B} \in \mathbb{R}^{(N-1) \times N}$ and feature matrix $\mathbf{F} \in \mathbb{R}^{(F+1) \times N}$ is $O((N-1)N(F+1))$. When the model is compact, only the first shape modes, or the first elements of matrix $\mathbf{B}$ are needed to describe a specific percentage of the shape variance, so $\mathbf{B}$ may be reduced to $\mathbf{B} \in \mathbb{R}^{K \times N}$. In that way, the complexity of the
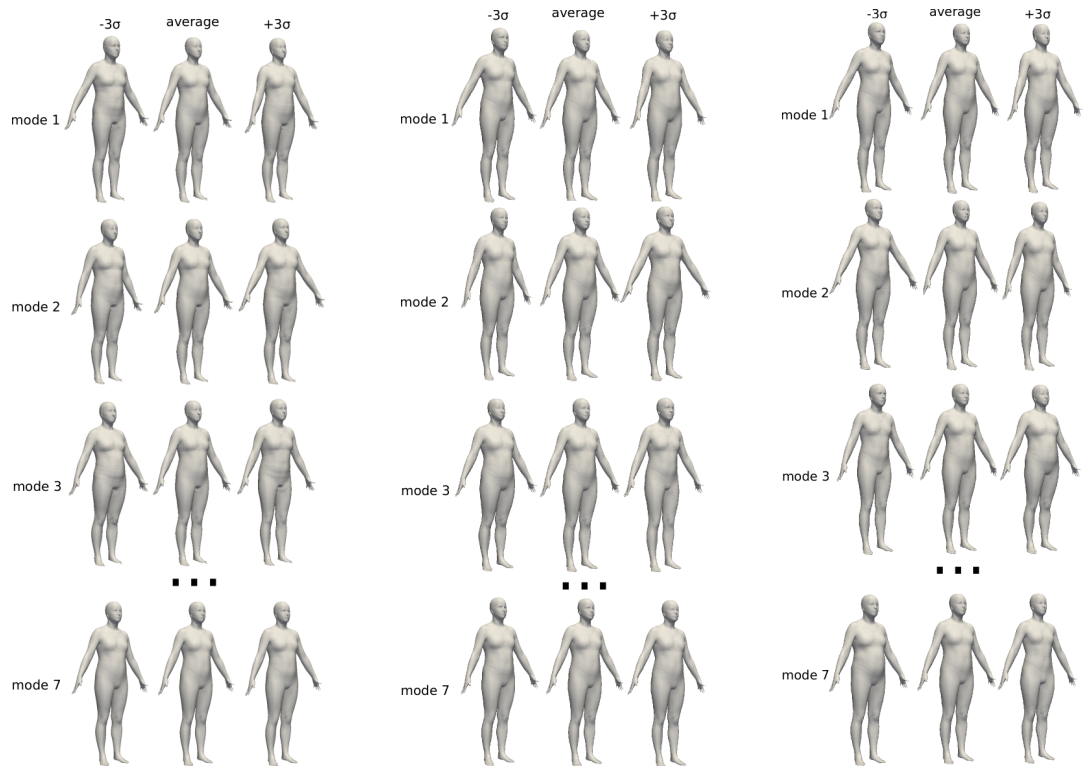
(a) Posture model using all features.

(b) Posture model using 11 best features.

(c) Posture model using 5 best features.
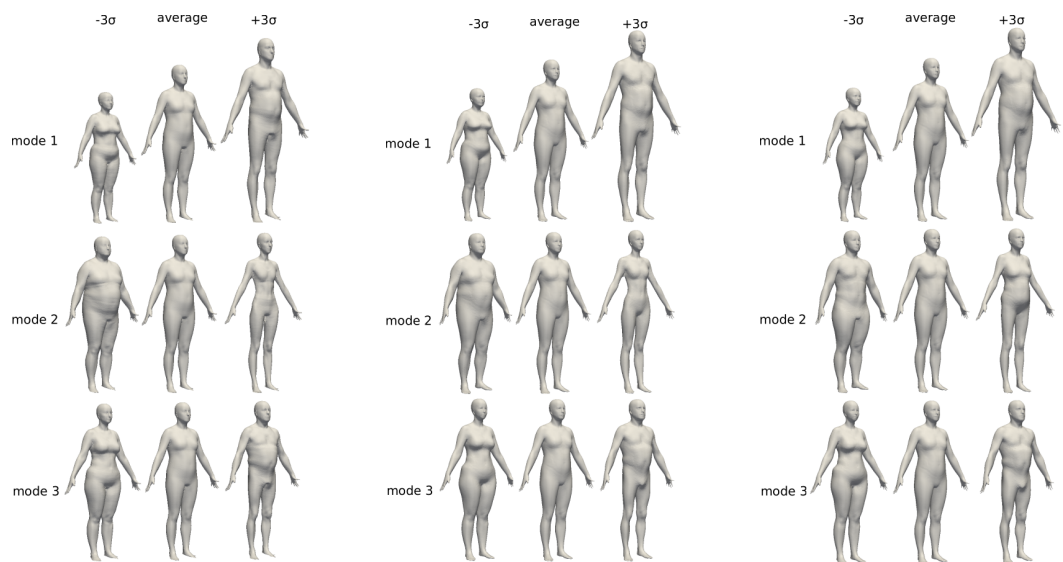
(d) Posture normalized SSM using all features.

(e) Posture normalized SSM using 11 best features.

(f) Posture normalized SSM using 5 best features.

**Figure 9.** Posture normalization with varying number of features.

17

multiplication is reduced from $O((N-1)N(F+1))$ to $O(KN(F+1))$. Also, a more compact model will lead to less energy consumption. The energy efficiency is directly linked to the relative profit obtained by a reduced computation time. Furthermore, a compact model will decrease the risk of overfitting. The more shape modes present in the shape model, the worse the precision of the estimated shape model parameters.

Hardly any difference is noticeable between the posture normalized SSM using all features and the posture normalized SSM using the 11 best features. These features are: stature, breast circumference, thigh circumference, crotch height, hip circumference, age, arm length, sitting height, waist circumference, shoulder breadth, and knee height. Therefore, the approach is reproducible with another dataset and some simple meta-data. It may be noted that stature is the most important feature to predict a person's body shape. Using only 5 features, a vast difference in shape can be observed in the second shape mode. This is because too many shape differences were incorporated in the posture model and thus filtered out in the posture normalized SSM. In general, the more measures available, the better the identity of a shape can be removed, so the better the posture can be separated from the shape. But this does not imply that the algorithm will not work when some specific measures are missing.

A method for simulating a body shape from simple measurements is a valuable tool for product developers that design near-body products. With our technique, a virtual 3D mannequin can be created. Such tools (Digital Human Models - DHM) are already widespread, but are often an oversimplified representation of the population, based on 1D measurements, so 3D shape variation is not incorporated (Moes 2010; Blanchonette 2010; van der Meulen and Seidl 2007). The body shape is modified by scaling the body parts. Therefore, these DHMs are not as realistic as the models that can be created by using a posture normalized SSM. Because we use a data-driven technique, the whole variation within the complete shape population is captured and simulated shapes are a realistic representation of a body with those measurements. We showed that by posture normalization, the body shape prediction error can be reduced by 48% (from $12.95mm$ to $6,59mm$). The method is also useful to visualize feature percentiles. In Figure 10, we show some body shapes simulated from one given feature.

For validation of our proposed framework, we used the existing CAESAR database (Robinette, Daanen, and Paquet 1999). The subjects got strict posture instructions before scanning. Their feet had to be placed on foot outlines positioned $10cm$ apart at the inside of the heel and were positioned on the scanner platform at a $30°$ angle. The researchers used a $20cm$ long dowel to adjust the subject's arm position so the hands were $20cm$ away from the most lateral point of the hip/thigh area. The arms and wrists were kept straight and the palms of the hands faced the body, with fingers spread. They were instructed to stand straight and look straight ahead. Because of these instructions, little posture variances were observed. Especially in the legs area, almost no variances can be seen. If the subjects from the CAESAR dataset would have been scanned with less strict instructions, more posture variation (e.g. angle between the legs, angle between the arms and the body, bending of the knees) would have been observed, leading to a posture model that is able to filter out more posture variation. Another option would be to generate a dataset with explicitly different postures, to assure a more robust normalization algorithm for large posture variations. More research is needed to see how a posture model built from a different dataset with more posture variation could cope with larger posture differences. We predict that finding correspondences between two body shapes with large differences in posture, will be the most challenging part.
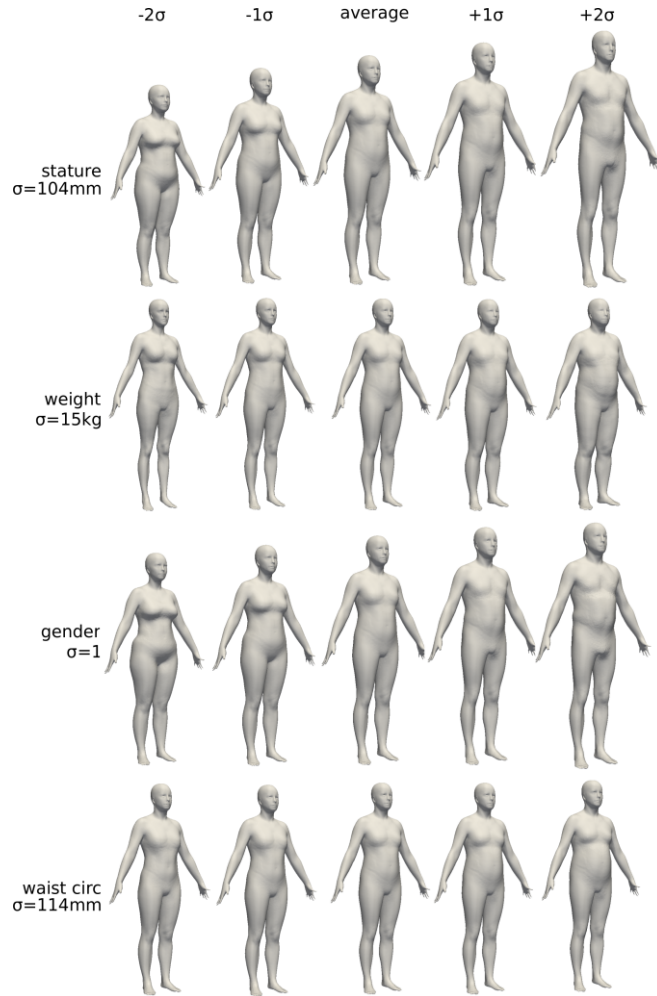
**Figure 10.** The most plausible body shapes from one given feature. The standard deviation $\sigma$ of the feature is calculated and the body shape is simulated for $-2\sigma$, $-1\sigma$, the average body shape $\mu$, $+1\sigma$ and $+2\sigma$.

Note that in this manuscript, all posture deviations were filtered out. This means that posture deviations related to natural posture are filtered out as well. In some cases, the influence of those posture deviations on the shape, is valuable information. A possible approach to keep these specific variations, is to look into detail to the shape modes of the posture model, and manually removing modes that have to do with natural posture variation. In other words, the user may choose to keep the mode of bending and flexing the arms, while removing the mode where the spine goes from kyphosis to lordosis, as this is related to natural posture. However, differentiating between unique postures and erroneous postures may require biomechanical insight of the posture variations.

One limitation of the described framework is that it uses a linear methodology. Therefore, it can not handle large rotational posture differences, such as torso flexion and rotation of the elbow. Our algorithm is able to correct for rotational deformations (to a certain accuracy) using multiple shape modes, as shown in Fig 6. Further investigation is needed to be able to cope with this type of posture differences.

A logical next step in this work, is adding motion to the statistical shape model. In that way, the shape model would be usable for reachability tests (e.g. when designing a

vehicle, to test whether the driver is able to reach everything) or designing near-body products (e.g. to test whether the clothes will fit the user, and to validate this for a whole range of motions).

The software for the described algorithms was written in Python and based on the Visualization ToolKit (VTK) libraries (Schroeder, Martin, and Lorensen 2002) and the Scientific Python (SciPy) libraries (Oliphant 2007). VTK is an open-source software systems for 3D computer graphics, image processing, and visualization. SciPy is a scientific computing library.

## 5. Conclusions

In this work, a new technique to perform statistical shape analysis in a posture-invariant way was proposed. Posture normalization allows to study shape variation that appears in a dataset of 3D body scans, despite the slightly varying postures of the individuals. With the posture model, any shape that is corresponded with the model can be normalized in a fast and precise way.

From the results we learn that applying statistical shape analysis on shapes normalized for posture results in more body shape related variations compared to performing the same shape analysis to non-normalized shapes. Because there is less shape variation present in the posture normalized population, a posture normalized SSM is a more compact representation of the population. Hence, less shape modes are necessary to describe a certain percentage of the population.

In short, our posture normalized SSM is a valuable tool to generate more realistic virtual design mannequins that can be exploited to design better ergonomic products. Furthermore, it is a beginning towards shape analysis of body scans in different poses, such as predicting a body shape in seated pose from a body shape in standing pose. As a result, only one scan would be sufficient to design products that require the body shape to be in another pose than the standard pose.

## Funding

## References

Anguelov, D., P. Srinivasan, D. Koller, S. Thrun, J. Rodgers, and J. Davis. 2005. "SCAPE: Shape Completion and Animation of People." *ACM Transactions on Graphics* 24 (3): 408.

Baran, I., and J. Popović. 2007. "Automatic rigging and animation of 3D characters." *ACM Transactions on Graphics* 26 (3): 72.

Blanchonette, P. 2010. "Jack Human Modelling Tool: a Review." *Air Operations Division. Defence Science and Technology Organisation, Tech. Rep. DSTO TR 2364* .

Bragança, S., P. Arezes, M. Carvalho, and S. Ashdown. 2016. "Effects of different body postures on anthropometric measures." *Advances in Ergonomics in Design: Proceedings of the AHFE 2016 International Conference on Ergonomics in Design* 485: 313–322.

Chen, Y., Z. Liu, and Z. Zhang. 2013. "Tensor-based human body modeling." In *Computer Society Conference on Computer Vision and Pattern Recognition*, 105–112. IEEE.

Danckaers, F., T. Huysmans, D. Lacko, A. Ledda, S. Verwulgen, S. Van Dongen, and J. Sijbers. 2014. "Correspondence preserving elastic surface registration with shape model prior." In *International Conference on Pattern Recognition*, Stockholm, Sweden, 2143–2148. IEEE.

Danckaers, F., T. Huysmans, D. Lacko, and J. Sijbers. 2015. "Evaluation of 3D Body Shape Predictions Based on Features." In *International Conference on 3D Body Scanning Technologies*, Ascona, Switzerland, 258–265.

Danckaers, Femke, Toon Huysmans, Ann Hallemans, Guido De Bruyne, Steven Truijen, and Jan Sijbers. 2018. "Full Body Statistical Shape Modeling with Posture Normalization." In *The 8th International Conference on Applied Human Factors and Ergonomics (AHFE 2017)*, Vol. 591, Los Angeles, California, USA, 437–448. Springer, Springer.

Davies, R. H., C. J. Twining, T. F. Cootes, J. C. Waterton, and C. J. Taylor. 2002. "A minimum description length approach to statistical shape modeling." *IEEE Transactions on Medical Imaging* 21 (5): 525–537.

Moes, N. C C M. 2010. "Digital human models: an overview of development and applications in product and workplace design." In *International Symposium on Tools and Methods of Competitive Engineering*, Ancona, Italy, 73–84.

Mohr, A., and M. Gleicher. 2003. "Building efficient, accurate character skins from examples." *ACM Transactions on Graphics* 22 (3): 562.

Oliphant, T. E. 2007. "Python for scientific computing." *Computing in Science and Engineering* 9 (3): 10–20.

Park, B. K., J. C. Lumeng, C. N. Lumeng, S. M. Ebert, and M. P. Reed. 2015. "Child body shape measurement using depth cameras and a statistical body shape model." *Ergonomics* 58 (2): 301–309.

Park, B. K., and M. P. Reed. 2015. "Parametric body shape model of standing children aged 3 - 11 years." *Ergonomics* 58 (10): 1714–1725.

Pishchulin, L., S. Wuhrer, T. Helten, C. Theobalt, and B. Schiele. 2017. "Building statistical shape spaces for 3D human modeling." *Pattern Recognition* 67: 276–286.

Reed, M.P., B-K. D. Park, and B.D. Corner. 2016. "Predicting seated body shape from standing body shape." In *International Digital Human Modeling Conference*, Montreal, Canada, 1–5.

Robinette, K.M., H. Daanen, and E. Paquet. 1999. "The CAESAR project: a 3-D surface anthropometry survey." In *International Conference on 3-D Digital Imaging and Modeling*, 380–386. IEEE Comput. Soc.

Schroeder, W, K Martin, and B Lorensen. 2002. *The Visualization Toolkit - an bbject-oriented approach to 3D graphics*. Kitware.

Su, Z. 2011. "Statistical shape modelling : automatic shape model building." PhD diss., University College London.

Valette, S., J. M. Chassery, and R. Prost. 2008. "Generic remeshing of 3D triangular meshes with metric-dependent discrete voronoi diagrams." *IEEE Transactions on Visualization and Computer Graphics* 14 (2): 369–381.

van der Meulen, P., and A. Seidl. 2007. "RAMSIS The Leading Cad Tool for Ergonomic Analysis of Vehicles." In *Digital Human Modeling*, Beijing, China, 1008–1017. Springer Berlin Heidelberg.

Vitronic. 1994. "Inhalte Lightbox - VITRONIC - the machine vision people." Accessed 2018-03-22. https://www.vitronic.com/3d-body-scanner/3d-scan-for-3d-printing/vitus-bodyscan-benefits-3d-printing/inhalte-lightbox.html.

Wold, H. 1973. "Nonlinear Iterative Partial Least Squares (NIPALS) Modelling: Some Current Developments." In *Multivariate AnalysisIII*, 383–407. Elsevier.

Wuhrer, S., C. Shu, and P. Xi. 2012. "Posture-invariant statistical shape analysis using Laplace operator." *Computers and Graphics (Pergamon)* 36 (5): 410–416.